Raising Flight Crews Aircraft Energy Awareness Through High Energy-Limit Trajectories

Ramon Andreu Altava, Jean Claude Mere, Pierre Neri, Daniel Delahaye, Thierry Miquel

Improving Flight Crews Aircraft Energy Awareness Through High Energy-Limit Trajectories

Ramon Andreu Altava *, Jean Claude Mere† and Pierre Neri‡
Airbus Operations SAS, Toulouse, 31300, France

Daniel Delahaye§ and Thierry Miquel¶
ENAC, University of Toulouse, 31400, France

The increased number of daily flights in the last decades has led to the densification of majors airports and the proliferation of air traffic delays. The approach phase is inherently complex and labor-extensive for flight crews, whose mission is to follow a stabilized approach. Current Flight Management Systems do not provide much help in situations of high energy, where crews apply challenging energy management techniques to land in the destination runway. Go-around procedures shall be initiated as soon as the aircraft is not at the correct energy condition at the stabilization gate, despite the increase of workload this type of operation induces to crews and air traffic controllers. The continuation of a non-stabilized approach may put at peril the safety of flight. This paper presents an algorithm that computes the trajectory that stabilizes the aircraft in the minimum distance, also known as high energy-limit trajectory. The provision of this trajectory contributes to raise flight crews awareness of aircraft energy state, and also to inform that stabilization is not possible and give the minimum distance to follow a stabilized approach. Flight simulator results helped to assess the operational concept and improve representativeness of real flight operations. The calculation of the trajectory on a real-time basis provides flight crews with useful information of aircraft energy condition, which improves flight safety and may ultimately reduce the number of non-stabilized approaches and go-around procedures.

Nomenclature

CI	=	Cost Index [kg/min]
Conf	=	Flap setting [−]
D	=	Aerodynamic drag force [N]

*PhD candidate, Navigation Systems, Airbus.
†Flight Management System engineer, Navigation Systems, Airbus.
‡Flight Management System engineer, Navigation Systems, Airbus.
§Head of Optim group, ENAC.
¶PhD, Optim group, ENAC.

dh	=	Altitude step [m]
ESF	=	Energy Share Factor $[-]$
E_{T_s}	=	Specific total energy [m]
E_{k_s}	=	Specific potential energy [m]
E_{p_s}	=	Specific kinetic energy [m]
FF	=	Fuel flow [kg/s]
g_0	=	Gravitational constant, 9.80665 [m/s^2]
h	=	Geometric altitude [m]
m	=	Aircraft mass [kg]
M	=	Mach [-]
s	=	Aircraft ground distance [m]
t	=	Flight time [s]
Thr	=	Thrust force [N]
TSP	=	Thrust Setting Parameter $[-]$
V	=	True airspeed [m/s]
V_w	=	Wind airspeed [m/s]
$\dot{V}$	=	Aircraft acceleration [m/s^2]
δ_{ab}	=	Airbrakes position $[-]$
Δ_{LG}	=	Landing gear position $[-]$
γ	=	Aerodynamic flight path angle [rad]
γ_T	=	Total flight path angle [rad]

I. Introduction

Air traffic doubles every 15 years and has proven to be resilient to external economic and geopolitical factors [1]. The increased number of flight operations implies the congestion of continental areas and saturation of major airports, leading to the proliferation of air traffic delays [2]. Safety levels have been improved over the years, since 2016 [3] registered the least amount of fatal accidents per million departures while 2017 registered the lowest number of fatalities [4]. However, the increased number of flights seems to be followed by a rise of serious incidents, most of them related to runway excursions issues. The distribution of accidents per flight phase for the last 10 years depicts that 35% of fatal accidents [4] occur during approach and landing phases. Flight crews shall decide to abort the landing and go around as soon as the aircraft is not stabilized for landing. On average, go-around procedures occur around 1 to 3 times every 1000 flights according to the analysis conducted by the Flight Safety Foundation [5]. Although the occurrence rate indicates that this type of operation is rare, the study suggests that compliance with go-around policy could have prevented some accidents in the past. In general, this type of safe procedures increases the workload of both pilots and air traffic controllers (ATCOs), reduces the capacity of the airport terminal area and contributes to the propagation of delays. Hence, flight crews avoid as much as possible to go around, maintaining the energy of the aircraft close to acceptable levels.

The stabilization criterion defines a set of conditions that have to be satisfied, otherwise landing should be aborted. In general, the flight shall be stabilized at a height of 1000 feet above the runway [6], with aircraft on the right flight path, in landing configuration and at airspeed close to the approach speed [7]. In particular, the 1000 feet height shown in Fig. 1 is used in Flight Management System (FMS) design. According to airline policies and type of approach (e.g. instrument or visual meteorological conditions), this condition may be different.

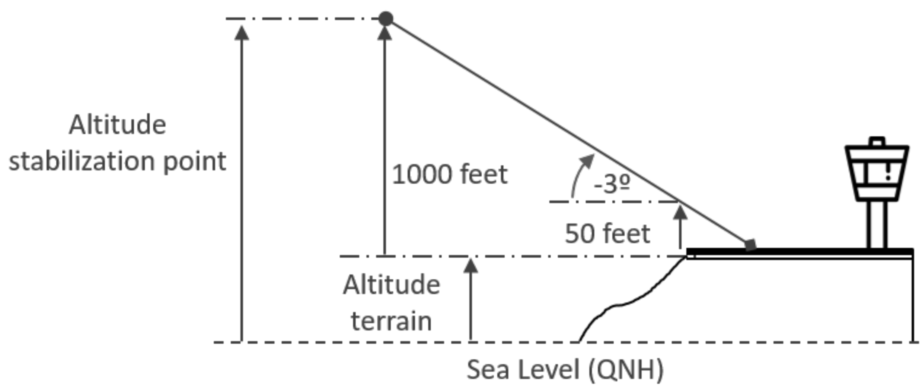

Fig. 1 Definition of the stabilization point.

The energy condition of an aircraft is defined as the sum of potential and kinetic energy. The concept of aircraft energy management refers to the continuous transformation of energy that occurs due to the use of flight and power controls as aircraft approach to the destination. Flight crews monitor the energy condition and ensure, through flight and power controls, that the altitude and the speed remain within reasonable limits. In automatic modes, FMS provides guidance commands with the aim of reducing the energy deviation and track the vertical profile computed by the system [8]. However, in manual modes, the reference profile is often not valid as the aircraft has deviated from the initial flight plan for some reason. In that case, pilots are responsible for the correct management of aircraft energy, which is done by means of power and control devices such as thrust levers, airbrakes, landing gear and flap settings. The most common causes for deviations from the profile computed by the FMS are late ATCOs clearances for landing, radar vectoring techniques, changes of landing runway, unaccounted winds and aircraft performance degradation. In approach phase, the previous factors may lead to an energy condition where the aircraft is above or below the intended energy profile. In low-energy conditions, aircraft are too low or too slow whereas in high-energy aircraft are too high, too fast or both.

While the former condition is easily recovered through extra thrust, high-energy requires to concatenate flight control actions with the aim of increasing the energy dissipation. The inherent workload during approach phase and the absence of assistance from the avionics systems as soon as aircraft are off path cause trouble to manage efficiently the aircraft energy. The provision of additional aircraft energy-related information could improve the situational awareness of flight crews and predictability of the trajectory for Air Traffic Control (ATC).

The topic of energy management during approach phase has been object of research during years from different perspectives. The formulation of the problem [9] [10] and the physics behind energy management [11] have been particularly discussed in [12][13]. Other works introduce the total energy angle [14], which is added for visualization on the primary flight display (PFD), and completes the flight information with the aim of improving flight crews energy awareness. However, these works focus more on human-machine interface, automation [15] and workload assessment than in trajectory optimization. On the ATC side, researches focus on data-driven algorithms to detect, at early stage, non-stabilized and non-compliant approaches [16][17]. Low-Noise Augmentation System (LNAS) [18] is an application on-boarded in an electronic flight bag (EFB) with the purpose of providing pilots with a dynamic computation of flap changes, gear and airbrakes extension. Flight tests have demonstrated that noise levels are reduced, altogether with fuel savings. Similary, the algorithms presented in [19] [20] also focus on optimizing the landing profile to minimize noise pollution. Furthermore, other energy-state approximations aim to compute optimal landing trajectories by optimizing the energy profile [21] [22]. The previous works address the problem from different perspectives to compute optimal landing trajectories. However, these works do not really deal with such high-energy scenarios where a solution does not exist. Thus, the domain of application of those algorithms could be enlarged with a pilot decision-tool aid dedicated to those situations where the vertical trajectory fails to solve the over-energy. This is the goal of this paper, which proposes an algorithm that computes the trajectory that stabilizes the aircraft in the minimum ground distance, also called the high energy-limit trajectory. The comparison between the computed minimum distance and the remaining distance from the aircraft position to the destination gives the path stretching distance to follow a stabilized approach. Similarly, this minimum distance could also be used to alert pilots to the proximity of the limit distance to perform a stabilized final approach. In both cases, the availability of this distance to crews raises awareness about aircraft energy with the aim of reducing the number of non-stabilized approaches, go-around procedures and eventually incidents related to energy mismanagement at landing.

The paper is structured as follows: the mathematical formulation of the problem is given in section II. The design of the algorithm that computes energy-limit trajectories is presented in section III. Then, section IV presents case studies of the high-energy limit trajectory, which have then been tested in Airbus flight simulators to assess the operational representativeness. The visualization and interpretation of the minimum distance provided by the algorithm is also presented. Finally, section V draws the conclusions of the study and discusses the integration of the concept in future flight operations.

II. Mathematical Formulation

A. Optimization Problem

The aircraft motion in the vertical plane is represented by a point-mass model, which provides a fair compromise between representativeness [23] and computing performance. The energy-limit trajectory stabilizes the aircraft in the minimum ground distance for any wind condition, and then provides the maximum energy dissipation in the shortest distance. Therefore, the objective function shall be written as follows:

$$J = \min \int_{h_0}^{h_f} \frac{V \cos\gamma + V_w}{V \sin\gamma} \, dh \tag{1}$$

The computation is performed upstream (i.e. backwards from the stabilization gate) to ensure that the aircraft meets the stabilization point at the correct energy condition. The independent variable is the aircraft altitude h whose value is bounded between h_0, which corresponds to the altitude at the stabilization point, and h_f, which is the aircraft current altitude. The algorithm computes the optimal trajectory by means of a genuine Airbus Performance database (PDB) that contains engine, aerodynamic and performance data.

B. Aircraft Model

The PDB contains the engine, the aerodynamic and the performance model for a certain aircraft type (see Fig. 2). This database is recurrently used by the algorithm for the computation of the energy-limit trajectory.

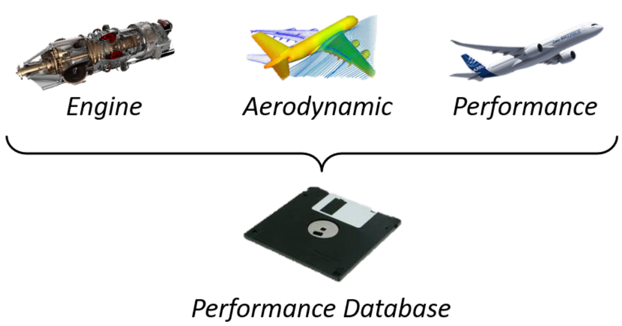

Fig. 2 Models contained into a FMS performance database.

High-energy conditions imply that engines are set to idle in order to minimize the total energy of the aircraft. Thrust setting parameter (TSP) values are function of altitude and speed:

$$TSP_{idle} = f_1(h, M) \tag{2}$$

Then, using the value obtained from Eq.(2), the thrust minimum rating for an engine idling is obtained:

$$Thr_{min} = f_2(TSP, h, M) \tag{3}$$

Besides, the fuel flow depends on TSP, altitude and speed:

$$FF = f_3(TSP, h, M) \tag{4}$$

The fuel flow is used to compute the variation of mass during the approach, although it has little influence in aircraft performance. This section presents a mathematical formulation based on the total energy of the aircraft, which relates aircraft altitude and speed states with the control variables. Aircraft specific energy is defined as the sum of kinetic and potential energies independent of aircraft mass. The derivation of the term with respect to time gives the energy rate or energy height of the aircraft:

$$\dot{E}_{T_s} = \dot{E}_{p_s} + \dot{E}_{k_s} = V \sin\gamma + \frac{V\dot{V}}{g_0} \tag{5}$$

Where g_0 is the gravitational acceleration and $\dot{V}$ is the acceleration of the aircraft. The energy rate defined by Eq.(5) is distributed between the potential and the kinetic energy. For doing so, the Energy Share Factor (ESF) is defined as the percentage of the total energy budget attributed to the kinetic energy whilst the remaining is allocated to the potential energy:

$$ESF = \frac{\dot{E}_{k_s}}{\dot{E}_{k_s} + \dot{E}_{p_s}} \tag{6}$$

The combination of Eqs.(5) and (6) leads to the following expression:

$$\sin\gamma = \frac{(1 - ESF)}{ESF} \frac{\dot{V}}{g_0} \tag{7}$$

The total flight path angle (γ_T) is the available energy budget independent of the aircraft airspeed. Therefore, it is represented as the sum of the aerodynamic flight path angle ($\sin\gamma$) and the resulting acceleration ($\dot{V}/g_0$):

$$\gamma_T = \sin\gamma + \frac{\dot{V}}{g_0} = \frac{\sin\gamma}{1 - ESF} = \frac{Thr_{min} - D(h, V, m, \delta_{ab}, \text{Conf}, \Delta_{LG})}{mg_0} \tag{8}$$

It is observed from Eq.(8) that the drag force depends on aircraft altitude h, true-airspeed V, aircraft mass m, airbrakes extension δ_{ab}, flap setting Conf and gear position Δ_{LG}. Since drag is higher than the minimum engine thrust, such that $D > Thr_{min}$, then $\gamma_T < 0$.

In this paper, the classic time-dependent equations of motion are converted into altitude-dependent, since the final altitude is known contrary to the final time and distance, this latter being the optimization variable. The combination of Eqs.(7) and (8) results in the following formulation:

$$\begin{cases} s' = \dfrac{ds}{dh} = \dfrac{V\cos\gamma + V_w}{V\sin\gamma} \\ V' = \dfrac{dV}{dh} = \dfrac{g_0\ ESF\ \gamma_T}{V\sin\gamma} \\ m' = \dfrac{dm}{dh} = \dfrac{-FF}{V\sin\gamma} \\ t' = \dfrac{dt}{dh} = \dfrac{1}{V\sin\gamma} \end{cases} \tag{9}$$

The prime symbol denotes the derivation with respect to altitude. Trajectory optimization problems focus on slow dynamics so that fast dynamics such the flight path angle has been neglected ($\dot{\gamma} = 0$). The equations of motion described in Eq.(9) define the state vector of the problem as:

$$x = [s, V, m, t] \tag{10}$$

Aircraft states are the consequence of the application of controls. The control vector for the energy-limit trajectory problem is defined as follows:

$$u = [ESF, \delta_{ab}, \text{Confaero}, \Delta_{LG}] \tag{11}$$

Where Δ_{LG} represents the decision of extending the landing gear, defined as a boolean depending on its position:

$$\Delta_{LG} = \begin{cases} 1 \rightarrow \text{gear down} \\ 0 \rightarrow \text{gear up} \end{cases} \tag{12}$$

Similarly to (12), flap changes are defined as a boolean, which represents the decision of flight crews to change or not the flap setting.

$$\text{Confaero} = \begin{cases} 1 \rightarrow \text{change} \\ 0 \rightarrow \text{no change} \end{cases} \tag{13}$$

It is noted that flap and gear decisions described in Eqs.(12) and (13) are irreversible, since the go-around trajectory is not considered.

C. Operational limitations

The operational restrictions depicted in this section bound the state and control variables of the optimization problem. The final approach fix (FAF) is usually defined by a waypoint containing an *AT* or *AT OR ABOVE* constraint:

$$\begin{cases} \text{AT OR ABOVE} \rightarrow \quad h \geq h_{CSTR} \\ \text{AT} \rightarrow \quad h = h_{CSTR} \end{cases} \tag{14}$$

The FAF is often limited by a speed constraint that limits aircraft speed below a certain value:

$$V_{CAS} \leq V_{CAS_{CSTR}} \tag{15}$$

Furthermore, ATC regulation generally imposes a maximum speed of 250 kt Calibrated Airspeed (CAS) for all aircraft below flight level (FL) 100:

$$V_{CAS} \leq V_{CAS_{SPDLIM}}, \quad \forall h \leq \text{FL100} \tag{16}$$

In clean flap configuration, aircraft speed is limited between the lowest selectable speed ($V_{LS} = 1.23V_{S1G}$) and the maximum operating speed (V_{MO}):

$$V_{LS} \leq V_{CAS} \leq V_{MO}, \quad \text{if Conf} = clean \tag{17}$$

However, during flap changes, the stall speed decrease and the speed shall remain between V_{LS} and the maximum flap extended speed (V_{FE}):

$$V_{LS} \leq V_{CAS} \leq V_{FE}, \quad \text{if Conf} \neq clean \tag{18}$$

The ESF distributes the aircraft energy loss ($Thr < D$) between the kinetic and the potential energy. Aircraft decelerations are more effective during level-offs as all the energy budget is dedicated to decelerate the aircraft. In order to reduce the number of combinations only three relevant ESF values are retained for the calculation:

$$ESF \in \{ESF|_{V_{CAS=const.}}, ESF|_{FPA=-3^\circ}, ESF|_{\text{level-off}}\} \tag{19}$$

Where:

- $ESF|_{V_{CAS=const.}}$ is defined as the energy repartition that permits to maintain current V_{CAS} speed.
- $ESF|_{FPA=-3^\circ}$ is the one that decelerates maintaining a -3° FPA.
- $ESF|_{\text{level-off}}$ corresponds to a decelerated level-off.

FPA is the aerodynamic flight path angle. True airspeed decreases as soon as altitude decreases, so that a certain deceleration is required to maintain constant calibrated airspeed. Regarding airbrakes extension, energy-limit trajectories require full airbrakes ($\delta_{ab_{\text{Full}}}$) as they generate more drag than any other deflection, so that:

$$\delta_{ab} \in \{0, \delta_{ab_{\text{Full}}}\} \tag{20}$$

However, airbrakes extension increases the stall speed V_{LS}, so their use is limited to clean and flap settings 1 and 2. Thus, airbrakes are inhibited for flap configurations 3 and Full:

$$\delta_{ab} = 0, \quad \text{if Conf} \geq 3 \tag{21}$$

Five different flap settings are considered for the landing aircraft:

$$\text{Conf} = \{\text{clean}, 1, 2, 3, \text{Full}\} \tag{22}$$

Finally, the deployment of landing gear is limited to a certain operational speed:

$$\Delta_{LG} = 0, \quad \text{if } V_{CAS} > 280\ kt \tag{23}$$

III. Trajectory Generator Algorithm

The algorithm implemented in this paper is a variation of the A* algorithm presented in [24] and [25] that computes fuel-efficient trajectories. In this case, the algorithm computes the shortest distance to stabilize the aircraft for a given aircraft altitude and speed. The energy-limit trajectory is not necessarily flown but informs flight crews of the aircraft energy condition. In previous works [**?**], the optimal trajectory linking the aircraft position to the runway threshold was found. However, in other situations, the aircraft may be in such high-energy condition that the stabilization is no longer possible. Under these circumstances, pilots may continue the approach, which will result in a non stabilization followed by a go-around procedure. This operation has a negative impact on workload, fuel consumption, noise and flight delays. The provision of additional energy information to flight crews could improve the energy awareness on a real-time basis with the aim of reducing the number of missed approaches. On that basis, the energy-limit trajectory could be continuously displayed to the pilot and be automatically activated as soon as the aircraft approximates the threshold. Therefore, the objective of the function is twofold: on one hand, it provides flight crews with a visualization of the limit trajectory enabling the stabilization. On the other hand, it provides pilots with the distance-to-stretch to stabilize the aircraft before landing in cases of strong over-energy. The calculation is performed backwards to ensure that the aircraft meets the correct state at the stabilization gate, and terminates at the current aircraft altitude and speed. The optimization variable being the ground distance, the algorithm provides the minimum distance for stabilization, in other words, the trajectory that gives maximum energy dissipation. This version of the algorithm is based on Dijkstra's algorithm [26] so that the heuristic function is zero for each node.

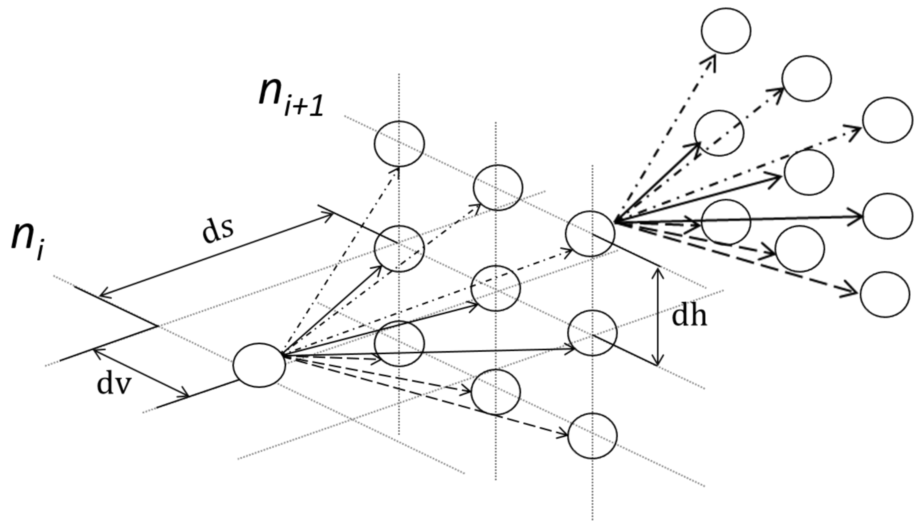

Fig. 3 Incremental generation of nodes based on discretized control values. The new states are compliant with all constraints, which are used for pruning the search space.

The search space is incrementally constructed from the initial node until reaching the current aircraft energy condition (see Fig. 3). At each iteration, new states are generated by using discrete control values. The different constraints such as altitude, speed or the glide path prune the search space and reduce the number of combinations of the optimization problem (see Fig. 4). The algorithm terminates as soon as a node located at the target altitude and speed provides the minimum ground distance. The projections of the optimal nodes in the XZ-plane yield the altitude profile (see Fig. 4(a)) whereas those projected on the XY-plane constitute the speed profile (see Fig. 4(b)). Since, the calculation yields the minimum ground distance to stabilize the aircraft independently of the aircraft distance to the runway, two scenarios are possible: in the case the aircraft distance to the destination is greater that the optimal value, the difference between both indicates the margin distance with respect to the energy-limit trajectory. Therefore, the aircraft shall continue the approach before reaching the minimum distance for stabilization. However, if the aircraft distance to the destination is shorter that the optimal value, the stabilization is not possible. The comparison between the optimal value and the aircraft position yields the minimum distance to stretch the lateral path. Different case studies with the correspondent evaluation in the Airbus flight simulator is provided in the next section.

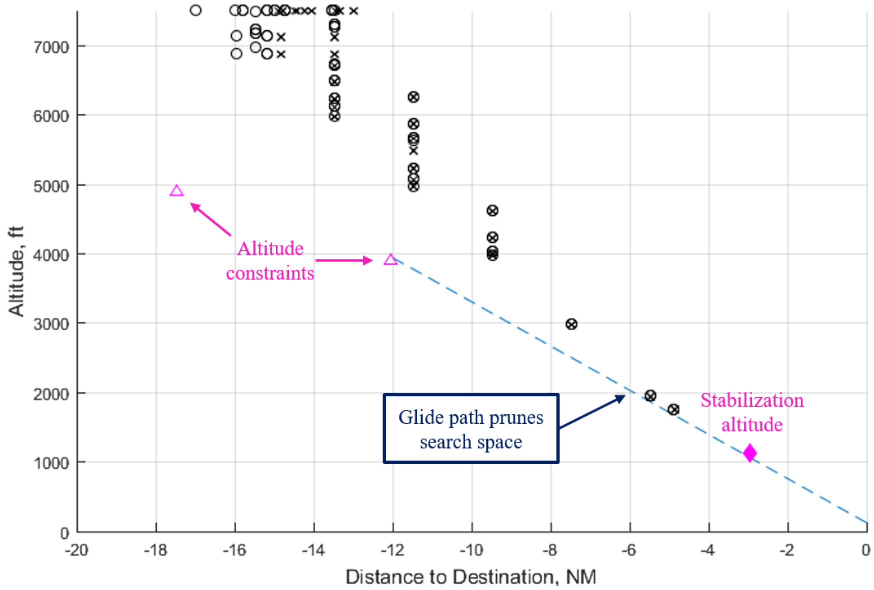

(a) Altitude profile on XZ-plane.

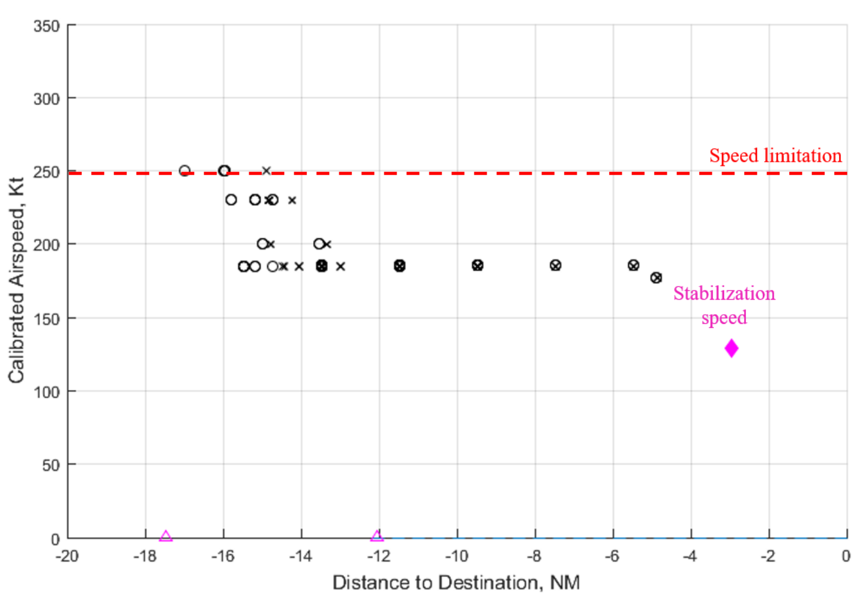

(b) Speed profile on XY-plane.

Fig. 4 Search space generation where states comply with all constraints. Any circle is a node that has been generated at some point whereas crosses represent nodes being expanded.

IV. Results and Findings

A. Computation of the high energy-limit trajectory

This section presents a case study where an aircraft is flying in normal condition but the clearance for landing has not yet been received. The computation of the trajectory informs pilots about the minimum ground distance that would result in a stabilized approach. The selected aircraft is the A320 NEO equipped with CFM engines. The aircraft landing gross weight is 60 tonnes, approximately 90% of its maximum landing weight (MLW). The aircraft lands in runway 24L at Los Angeles airport (KLAX). The aircraft flies in a level-off at constant speed, both the initial and the final state being summarized in the following table:

Table 1 Parameters of the simulation.

	Initial state	Final state
Distance to destination, NM	-2.95	s_f
Altitude, ft	1125	7500
Speed, kt	134.6	250
Flap settings	Full	Clean
Landing gear	Down	Up

Note that the computation is performed upstream so that the initial position corresponds to the stabilization gate and the final position is the current aircraft state without accounting for the distance to the destination.

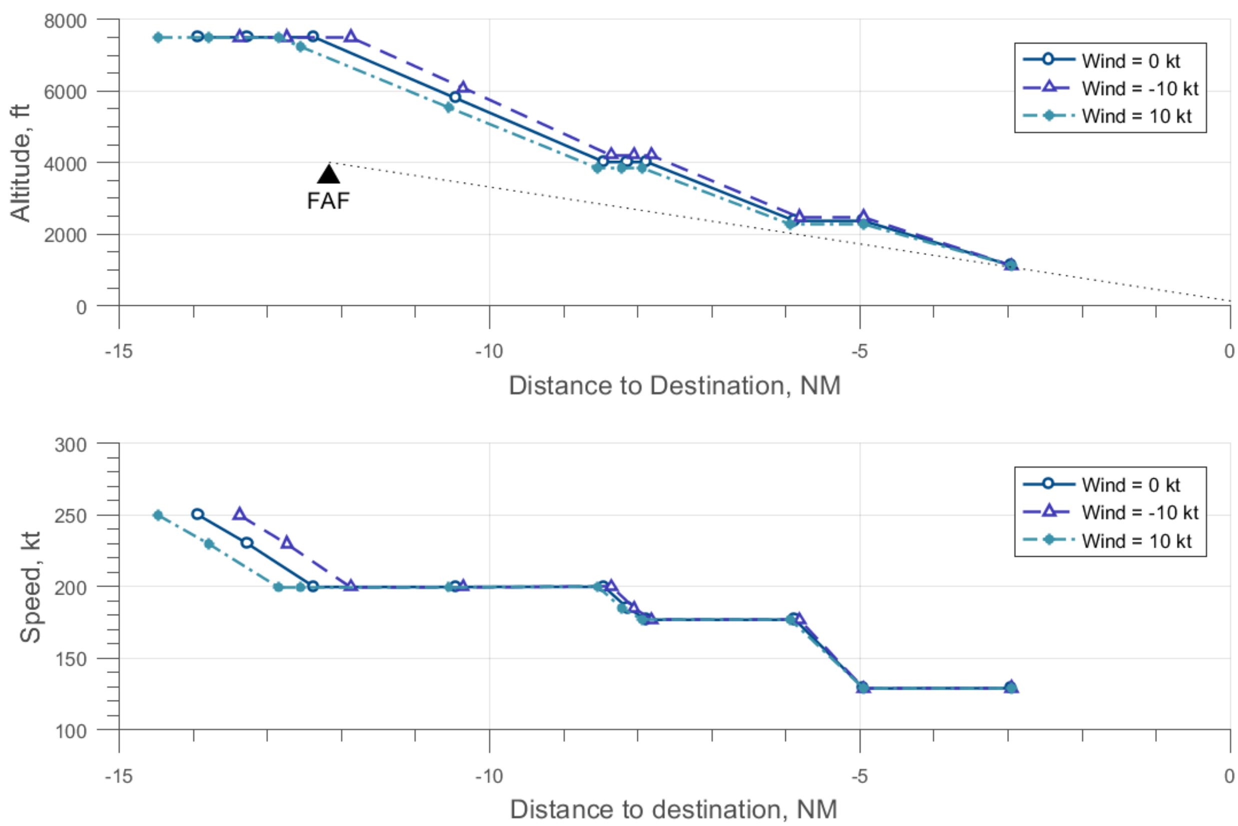

Fig. 5 Influence of constant winds in the computation of the energy-limit trajectory.

The influence of the wind in the trajectory is displayed in Fig. 5. In this case, three constant winds have been tested: zero wind, 10 knots of tailwind and 10 knots of headwind. The value of 10 knots represents the tailwind component limit for take-off and landing defined by the manufacturer for this type of aircraft. It means that stronger winds could be found at higher altitudes, but 10 knots of tailwind is the maximum magnitude that could be found when the aircraft is close to the runway. As it is observed in Fig. 5, a wind of 10 knots increases or decreases ground distance by ±4%, depending on the wind direction.

B. Case study I: Computation of high energy-limit trajectory

The analysis of the trajectory is performed for the zero wind case in order to disregard the wind effect on the minimum ground distance. Therefore, the altitude and speed profile of the energy-limit trajectory is shown in Fig. 6. Besides, it is observed from Fig.7 that the gear is set down and airbrakes are fully extended for the whole trajectory, as it provides the highest energy rate. Decelerations are performed in level-flight to increase the braking efficiency, and flap settings are changed at maximum speed (V_{FE}) to increase drag. The utilization of airbrakes increases the lowest selectable speed (V_{LS}), so their extension is inhibited in landing configuration. This results in a delay of full flap setting, since the aircraft generates more drag at flap setting 2 with airbrakes full extended than flying in landing setting and airbrakes inhibited. Nevertheless, the flap 3 change occurs at V_{FE}, instead to the lowest selectable speed, to prevent speed from falling into the stall area.

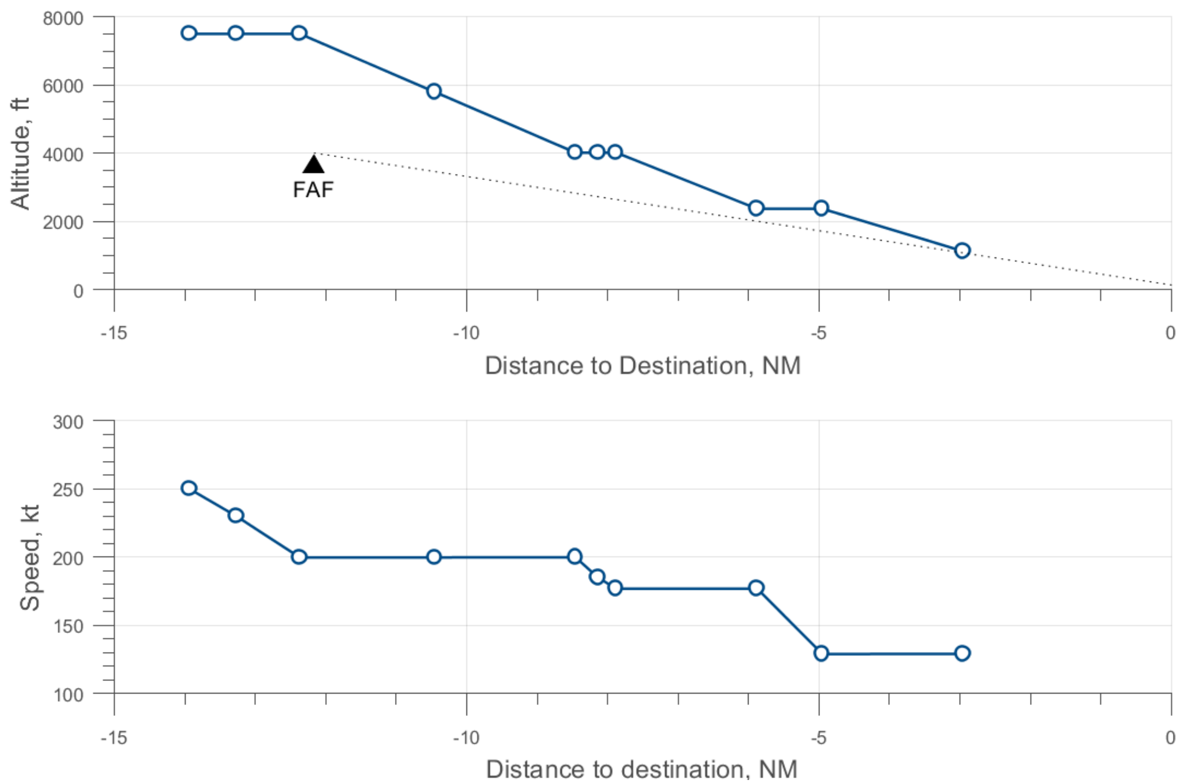

Fig. 6 Case study I: Altitude and speed profiles for the energy-limit trajectory.

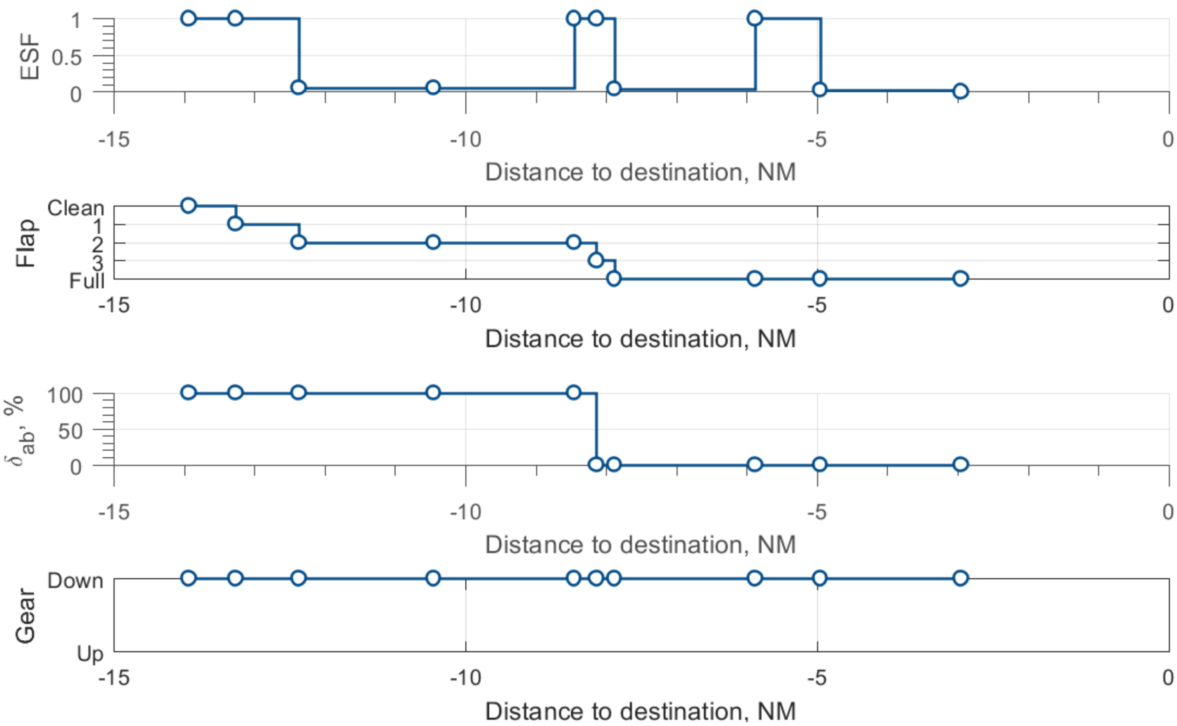

Fig. 7 Case study I: Values of control variables for the energy-limit trajectory.

C. Case study I: Flight simulator assessment

Flight simulations were conducted at Airbus facilities in order to evaluate whether the trajectory is flyable with current flight modes or not. The integration points used by the algorithm were inserted manually in the flight plan under the name of INTAXX (e.g. INTA10), so the actions were performed at the right moment. Figure 8 shows the Electronic Flight Instrument System (EFIS) and the Multi-Purpose Control Display Unit (MCDU) display during the simulator session, the former consisting of a Primary Flight Display (PFD) and Navigation Display (ND).

(a) PFD display. (b) ND display. (c) MCDU F-PLN page.

Fig. 8 EFIS and MCDU display during the simulation tests.

The auto-thrust was switched-off with thrust levers manually set at idle detent and the autopilot was engaged; the aircraft was on path aligned with the runway axis (see Fig.8(b)) and vertically guided by the FPA targets set in the flight control unit (FCU) and displayed on the flight mode annunciator (FMA) of the PFD, as shown in Fig.8(a).

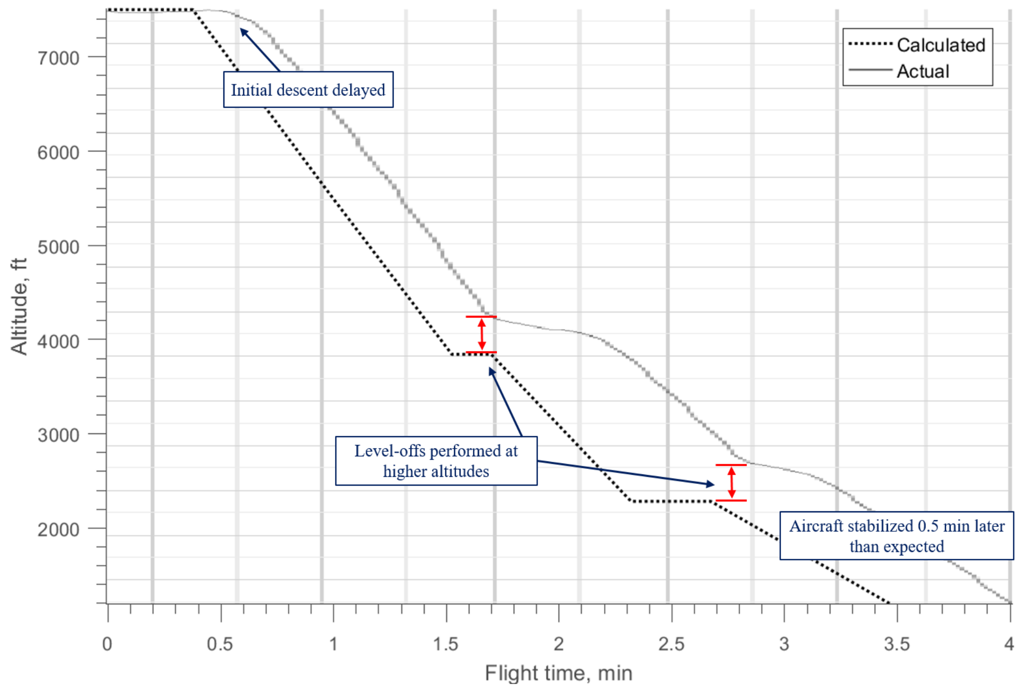

Fig. 9 Test 1: Comparison between the altitude profile calculated and the actual one flown in flight simulator.

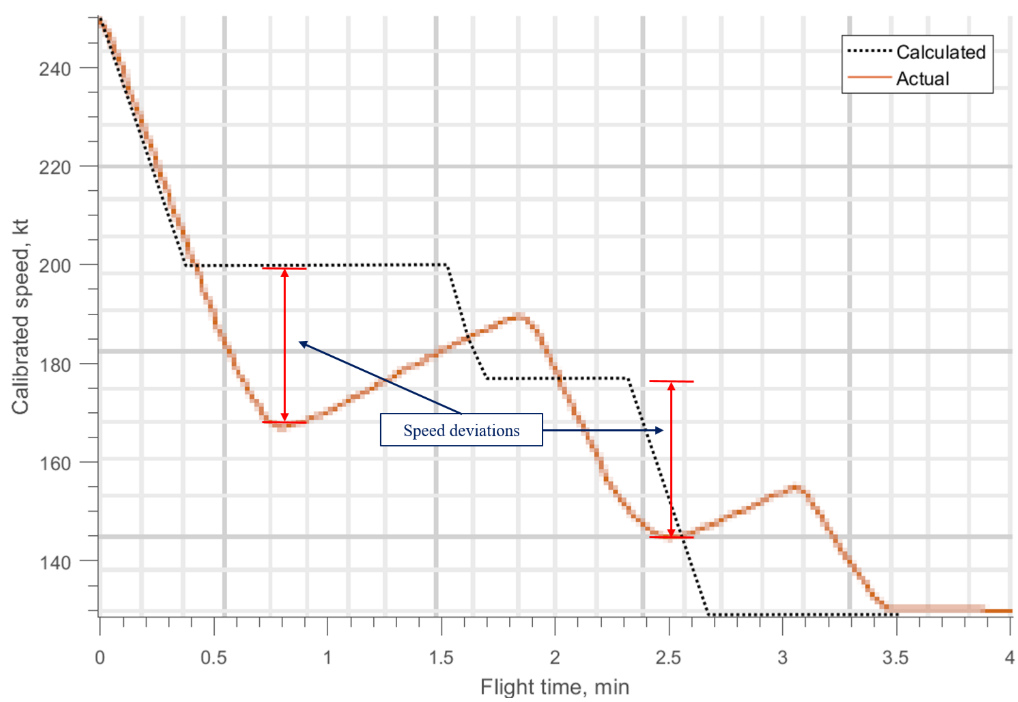

Fig. 10 Test 1: Comparison between the speed profile calculated and the actual one flown in flight simulator.

The feedback collected after the simulation session shows that the workload was reasonable, although deviations in the profile occurred as a result of delay in FPA changes. The guidance law transition between a shallow FPA (e.g. 0°) and a steep one (e.g. -7°) is not immediate and the aircraft over-shoots the calculated profile. Similarly, the aircraft under-shoots the altitude profile in the transition between steep paths and level-offs. The post-simulation data analysis confirms the feedback collected during the tests. As it is observed in Fig. 9, the aircraft over-shoots the profile and the deceleration continues. Then, an increase of FPA produces an increase of airspeed (see Fig. 10). The second level-off is anticipated although the aircraft still deviates the vertical profile. In reality, this level-off is so short that the guidance law hardly performs it. A similar situation occurs in the third level-off, where the aircraft is set in landing configuration. As a result, the aircraft arrives 1000 feet above the stabilization gate at approach speed. The approach is obviously non-stabilized and the aircraft shall go around under these circumstances.

The operational assessment of the function concluded that intermediate level-offs are undesirable and difficult to be followed by present flight controls and guidance laws. Thus, the previous calculation of the energy-limit trajectory is somehow theoretical, which needs refinements to improve the operational representativeness and facilitate the path-tracking. The definition of more reactive guidance laws could be a solution but would induce undesirable effects on passenger comfort due to sharp changes in normal acceleration ($\dot{\gamma}$). Therefore, the construction of a conservative energy-limit trajectory, which accounts for additional operational constraints, has been constructed and tested in the flight simulator.

D. Case study II: Computation of the high energy-limit trajectory with improved logics

The proposed trajectory is displayed in Fig. 6. This energy-limit trajectory requires 3% extra ground distance with respect to the one of Fig. 9. Intermediate level-offs except the initial deceleration segment have been removed. For doing so, it is assumed that the aircraft shall be on the glide path as soon as possible, so that flap changes 3 and Full occur during the glide on final approach. Besides, airbrakes extension is forbidden before reaching the glide slope, so crews can compensate any unexpected tailwind. These design choices aim at minimizing the under and over-shoots produced by abrupt changes of FPA, specially when these happen close to the stabilization gate in order to execute a safe landing. Regarding the control variables, gear is down for the full trajectory. Airbrakes are deployed until the transition segment to the glide slope. The impact of airbrakes in the descent path is observed in Fig. 11, where a change of flight path is produced as soon as airbrakes are retracted (see Fig. 12). It enables a smooth transition from -7.8° to -3° flight path. Then, on the glide path the aircraft sets the landing configuration, decelerating from 185 kt to 129 kt approach speed.

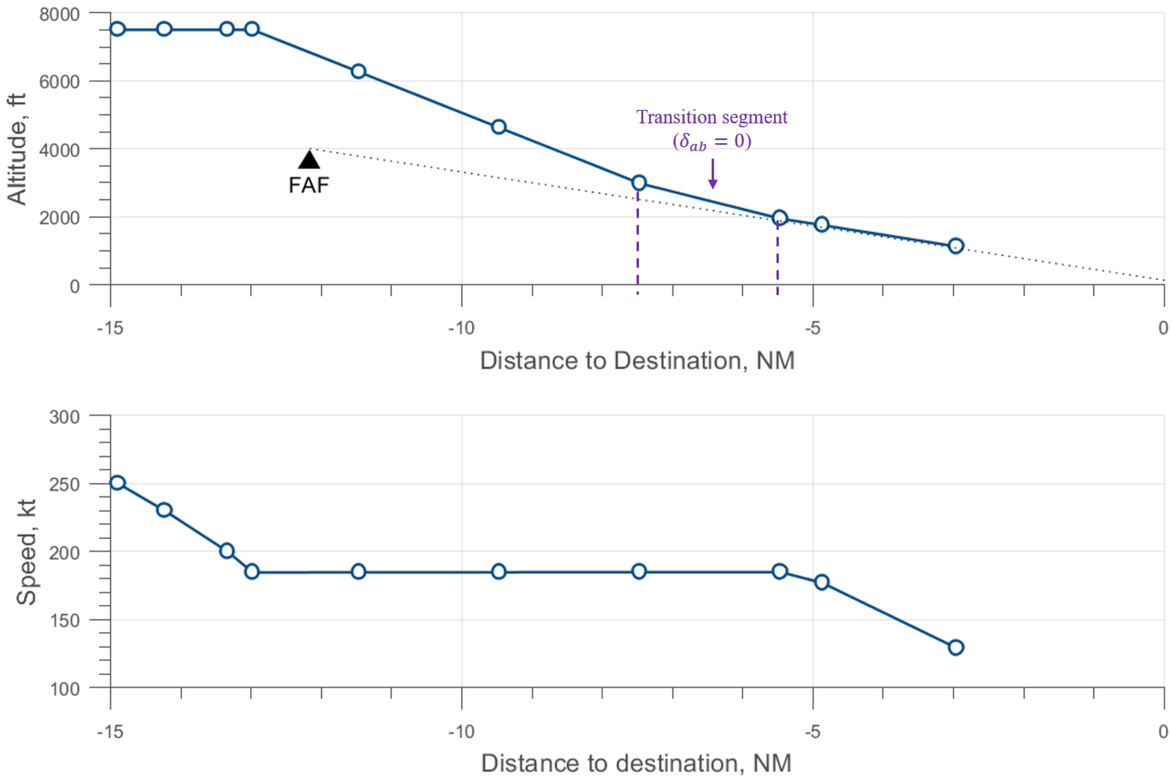

Fig. 11 Case study II: Altitude and speed profiles for the energy-limit trajectory.

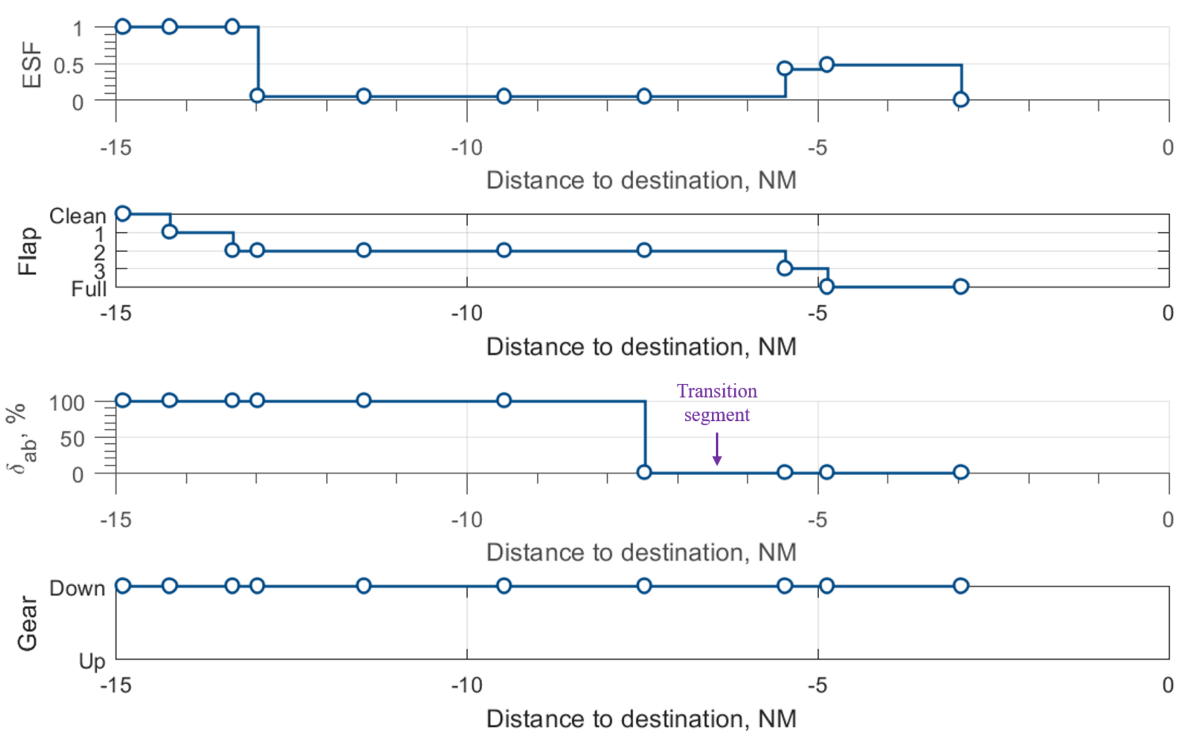

Fig. 12 Case study II: Values of control variables for the energy-limit trajectory.

E. Case study II: Flight simulator assessment

The second high energy-limit trajectory with improved logics was also tested in Airbus flight simulators. In this case, the path-tracking of the trajectory was easier than in the previous case. Also, workload was reduced as a result of the removal of intermediate level-offs. In the whole trajectory, only two FPA changes were performed. As it was observed during the session, this decrease of workload allowed to focus attention on the behavior of altitude and speed.

The post-session data analysis confirms the feedback collected during the simulation session. As it can be observed in Fig. 13, the altitude profile was accurately followed. Again, an over-shoot occurred at the beginning of the descent, which produced a decrease of airspeed that was quickly compensated by increasing the steep path. However, the speed was close to the stall speed, which could have activated the alpha-floor protection. Basically, if the aircraft is in nominal operation mode (e.g. no air data failure) and the speed drops close the stall speed, the alpha-floor protection engages the auto-thrust, sets maximum thrust and initiates a climb to recover the low speed situation. In general, the speed behavior was slightly different than calculated, as it is observed in Fig. 14. The speed dropped below 185 kt, then it increased to 190 - 195 kts, from where it was maintained until the aircraft reached the glide slope. At the end, both altitude and speed errors were very small. The aircraft followed the trajectory computed by the A* and met the stabilization gate at the right energy state. Although this energy-limit trajectory requires 3% extra distance with respect to the previous one, the operational representativeness has been largely increased as it has been proved during the tests.

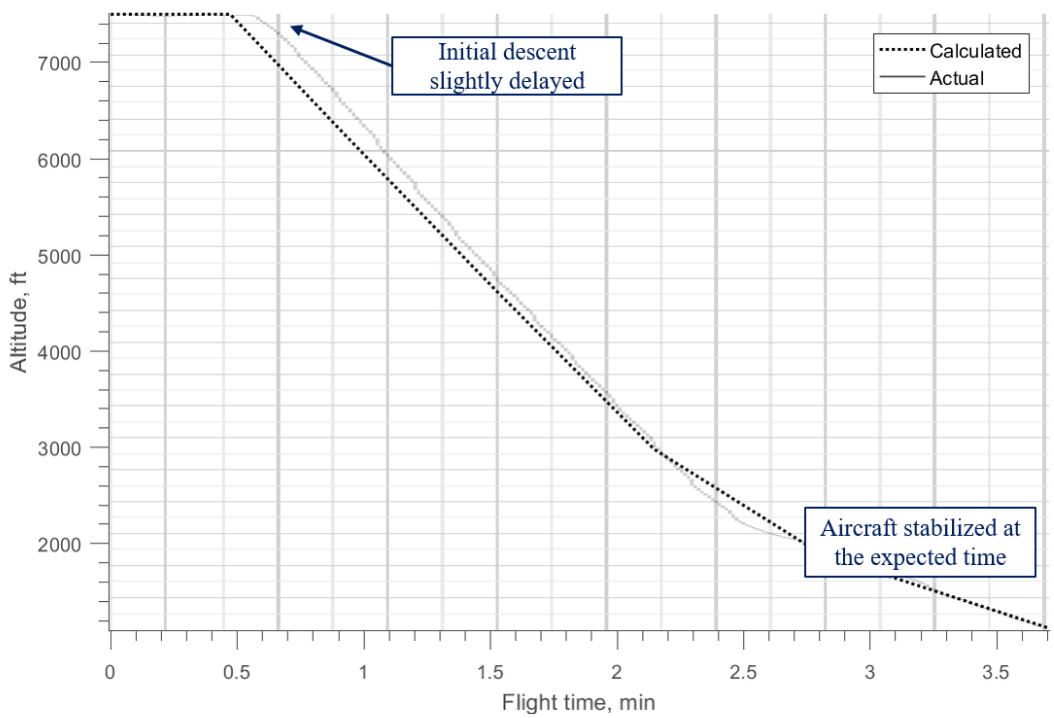

Fig. 13 Test 2: Comparison between the altitude profile calculated and the actual one flown in flight simulator.

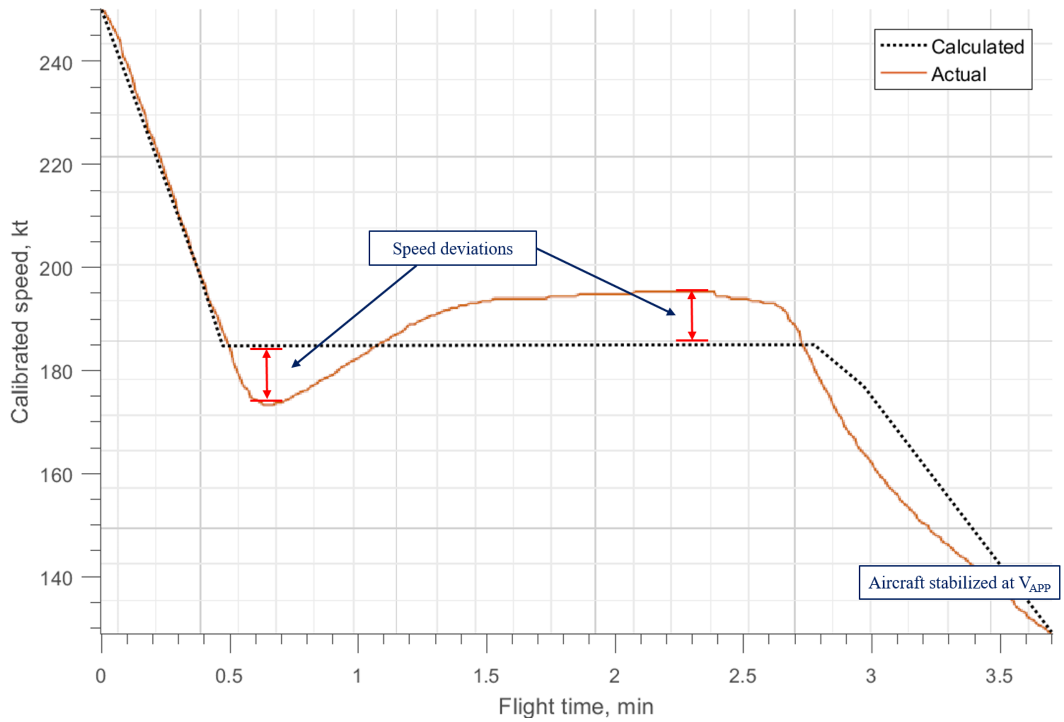

Fig. 14 Test 2: Comparison between the speed profile calculated and the actual one flown in flight simulator.

F. Flight crews use of the high energy-limit trajectory

The energy-limit trajectory provides the trajectory that stabilizes the aircraft in the minimum ground distance. This trajectory is a back-up calculation continuously displayed to crews in order to improve their awareness of the aircraft energy condition. The minimum ground distance provides a useful awareness of the aircraft energy with regard to the runway. On one hand, this distance alerts flight crews of the proximity of the zone from where the stabilization is unfeasible (see Fig. 15). On the other hand, in high-energy cases where stabilization is already unlikely, this distance is used as the minimum to stretch the path for stabilization. Flight crews do not need to resume their efforts on stabilizing the aircraft and could directly demand radar vectors to the ATC in order to reintegrate the aircraft arriving flow.

The visualization of the minimum distance given by the energy-limit trajectory can be done through an energy-arc whose center is at the stabilization gate. The integration points used for the computation are then displayed on the ND. The vertical trajectory could be displayed in the vertical display (VD) for those aircraft equipped with, or alternatively in an EFB. A simply interpretation of the energy-arc is provided in Fig. 16 for KLAX airport. The FAF waypoint and the -3 degree glide path on final approach are also displayed, which highlights how steep the energy-limit path is. The terrain data has been retrieved from [27]. On one hand, if the aircraft is behind the energy-arc, stabilization is still possible under the current energy condition. Energy margin for stabilization is reduced as soon as the aircraft gets closer to the energy-arc. On the other hand, the aircraft shall go around as soon as it enters in the energy-arc zone, since compliance with stabilization criteria is not possible.

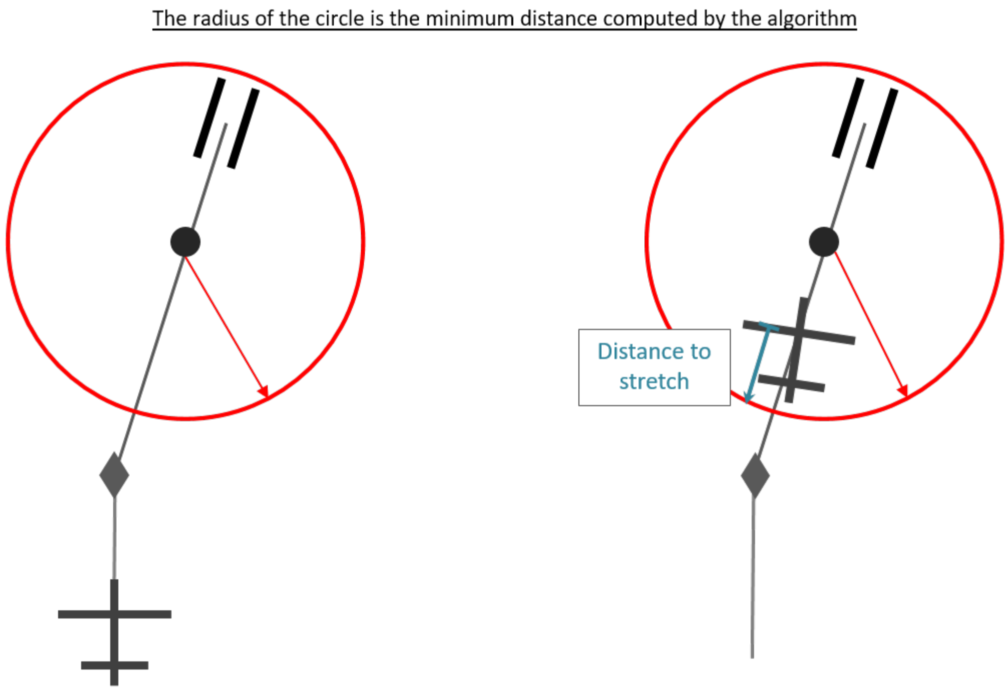

Fig. 15 Flight crews use of the energy-limit trajectory. The minimum ground distance is displayed as a circle whose center is a the stabilization gate. In the left, the aircraft is beyond the circle so that the stabilized approach is still possible. In the right, the aircraft is within the circle, the stabilization is no longer possible.

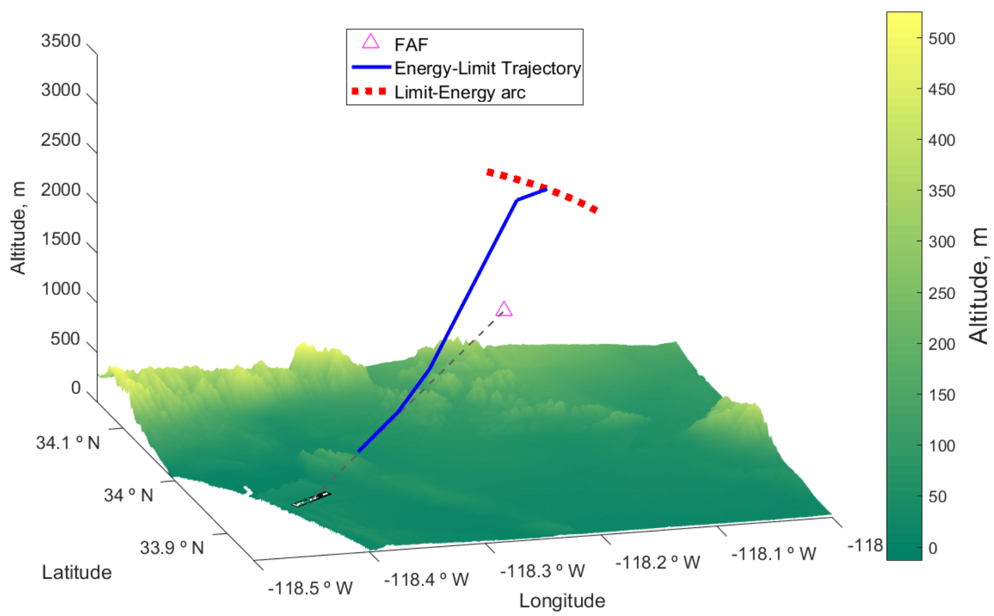

Fig. 16 High energy approach to KLAX 24L. The minimum distance is displayed as an energy-arc (red dashed line). The energy-limit trajectory is shown by a blue solid line above the glide path (gray dashed line).

V. Conclusion

This papers proposes an algorithm that computes the energy-limit trajectory, which is defined as the trajectory that stabilizes the aircraft in the minimum ground distance in compliance with airline policies. This trajectory provides the maximum energy dissipation accounting for the wind profile. Since state-of-the-art Flight Management Systems (FMS) provide little help to manage high-energy situations, the provision of the energy-limit trajectory is useful to: 1) improve flight crews awareness of current aircraft energy state to negotiate approach clearances with air traffic control (ATC). 2) It provides the minimum distance to stretch the lateral path to follow a stabilized approach, which avoids to continue a non-stabilized one and going around. Aircraft can reintegrate the arrival flow sooner, improving flight safety and minimizing the economic impact. The computed trajectories have been evaluated in flight simulators and demonstrate that they are flyable with current flight controls and guidance laws. Furthermore, the energy-limit trajectory could be displayed as an energy-arc whose radius is the minimum distance centered at the stabilization gate. It provides an easily interpretable aid to inform flight crews of the proximity of the non-stabilization zone or the minimum path stretching distance to stabilize the aircraft. In conclusion, energy-limit trajectories could help flight crews to manage aircraft energy in complex situations and also ATC to deal with non-stabilized approaches. As directions for future work, further investigation with flight test pilots and system experts, under different wind conditions, is recommended in order to increase the maturity of the algorithm and the operational representativeness of the computed trajectories before proceeding to flight tests.

References

[1] Airbus (ed.), *Global Market Forecast 2019-2038 - Mapping Demand*, Airbus S.A.S. ISBN: 978-2-9554382-4-6, 31707 Blagnac Cedex, France, 2019.

[2] Eurocontrol (ed.), *European Aviation in 2040. Challenges of Growth*, Eurocontrol, Brussels, 2018.

[3] ICAO, *State of Global Aviation Safety*, ICAO Safety Report, International Civil Aviation Organization, 999 Robert-Bourassa Boulevard, Montréal, Quebec, Canada H3C 5H7, 2019.

[4] EASA (ed.), *Annual Safety Review*, European Aviation Safety Agency, Koln, Germany, 2018.

[5] Blajev, T., and Curtis, C. W., *Go-Around Decision-Making and Execution Project*, Flight Safety Foundation, 2017.

[6] Airbus (ed.), *Flying Stabilized Approaches*, Flight Operations Briefing Notes, 2006.

[7] ALAR (ed.), *Stabilized Approach*, Flight Safety Foundation FSF ALAR Briefing Note 7.1, 2009.

[8] Avery, D., "The Evolution of Flight Management Systems," *IEEE Software*, Vol. 28 issue 1, Jan-Feb 2011, pp. 11–13. https://doi.org/10.1109/MS.2011.17.

[9] Cliff, E. M. (ed.), *Energy-State Models*, April 23, 1998.

[10] Zagalsky, N., “Aircraft energy management,” *AIAA 11^{th} Aerospace Sciences Meeting*, 1973. https://doi.org/10.2514/6.1973-228.

[11] Merkt, J. R., “Solving an Age-Old Debate: What Really Controls Altitude and Airspeed?” *Aerospace International Research Conference*, 2015.

[12] Merkt, J. R., “Flight Energy Management Training: Promoting Safety and Efficiency,” *Journal of Aviation Technology and Engineering*, Vol. 3, 2013, pp. 24–36. https://doi.org/10.7771/2159-6670.1072.

[13] Calise, A. J., “Extended Energy Management Methods for Flight Performance Optimization,” *13th Aerospace Sciences Meeting*, 1975. https://doi.org/10.2514/6.1975-30.

[14] van den Hoven, M., Borst, C., Mulder, M., and van Paassen, M., “Investigation of Energy Management during Approach - Evaluating the Total Energy-Based Perspective Flight-Path Display,” *TAIAA Guidance, Navigation, and Control Conference*, August 2010. https://doi.org/10.2514/6.2010-8401.

[15] Amelink, M. H. J., Mulder, M., van Passen, M., and Flach, J., “Theoretical Foundations for a Total Energy-Based Perspective Flight-Path Display,” *The International Journal of Aviation Psychology*, Vol. 15 No.3, July 2005, p. 205–231. https://doi.org/10.1207/s15327108ijap1503_1.

[16] Jarry, G., Delahaye, D., Nicol, F., and Féron, E., “Aircraft Atypical Approach Detection using Functional Principal Component Analysis,” *SESAR Innovations Days 2018*, 2018.

[17] Gong, C., and Sadovsky, A., “A Final Approach Trajectory Model for Current Operations,” *AIAA Aviation Technology, Integration and Operations (ATIO) Conference*, 2010. https://doi.org/10.2514/6.2010-9117.

[18] Abdelmoula, F., and Scholz, M., “LNAS - A Pilot Assistance System for Low-Noise Approaches with Minimal Fuel Consumption,” *31st Congress of the International Council of the Aeornautical Sciences*, 2018.

[19] Ohta, H., “Analysis of Minimum Noise Landing Approach Trajectory,” *Journal of Guidance, Control and Dynamics*, Vol. 5 No.3, 1982. https://doi.org/10.2514/3.56166.

[20] Fernandes, R., and Beskens, C., “Benefits of Optimal Flight Planning on Noise and Emissions Abatement at the Frankfurt Airport,” *AIAA Guidance, Navigation and Control Conference*, 2012. https://doi.org/10.2514/6.2012-4482.

[21] Zhao, Y., and Tsiotras, P., “Analysis of Energy-Optimal Aircraft Landing Operation Trajectories,” *Journal of Guidance, Control and Dynamics*, Vol. 36, No. 3, 2013. https://doi.org/10.2514/1.57779.

[22] De Jong, P. M. A., De Gelder, N., Bussink, F. J. L., Verhoeven, R. P. M., Kohrs, R., and Mulder, M., “Time and Energy Management during Descent and Approach for Aircraft: Batch-Simulation Study,” *Journal of Aircraft*, Vol. 52, No. 1, 2013. https://doi.org/10.2514/1.C032668.

[23] L.Schultz, R., and R.Zagalsky, N., “Aircraft Performance Optimization,” *Journal of Aircraft*, Vol. 9, No. 2, 1972. https://doi.org/10.2514/3.44326.

[24] Andreu-Altava, R., Mere, J., Delahaye, D., and Miquel, T., "Flight Management System Pathfinding Algorithm for Automatic Trajectory Generation," *37th Digital Avionics System Conference, London, UK*, 2018. https://doi.org/10.1109/DASC.2018.8569254.

[25] Andreu-Altava, R., Mere, J., Delahaye, D., and Miquel, T., "Graph-Search Descent and Approach Trajectory Optimization Based on Enhanced Aircraft Energy Management," *AIAA Aviation Forum 2019,*, 17-21 June 2019. https://doi.org/10.2514/6.2019-3618.

[26] E. Rippel, A. B.-G., and Shimkin, N., "Fast Graph-Search Algorithms for General Aviation Flight Trajectory Generation," *Journal of Guidance, Control and Dynamics*, 2005. https://doi.org/10.2514/1.7370.

[27] A., J., Reuter, H., Nelson, A., and Guevara, E., "Hole-filled seamless SRTM data V4, International Centre for Tropical Agriculture (CIAT)," *http://srtm.csi.cgiar.org*, 2008.